THE JOURNAL OF PHYSICAL CHEMISTRY B

Article

pubs.acs.org/JPCB

Hydrocarbons Depending on the Chain Length and Head Group Adopt Different Conformations within a Water-Soluble Nanocapsule: ^{1}H NMR and Molecular Dynamics Studies

Rajib Choudhury, Arghya Barman, Rajeev Prabhakar,* and V. Ramamurthy*

Department of Chemistry, University of Miami, Coral Gables, Florida 33124, United States

Supporting Information

ABSTRACT: In this study we have examined the conformational preference of phenyl-substituted hydrocarbons (alkanes, alkenes, and alkynes) of different chain lengths included within a confined space provided by a molecular capsule made of two host cavitands known by the trivial name "octa acid" (OA). One- and two-dimensional ^{1}H NMR experiments and molecular dynamics (MD) simulations were employed to probe the location and conformation of hydrocarbons within the OA capsule. In general, small hydrocarbons adopted a linear conformation while longer ones preferred a folded conformation. In addition, the extent of folding and the location of the end groups (methyl and phenyl) were dependent on the group (H_2C-CH_2, HC═CH, and C≡C) adjacent to the phenyl group. In addition, the rotational mobility of the hydrocarbons within the capsule varied; for example, while phenylated alkanes tumbled freely, phenylated alkenes and alkynes resisted such a motion at room temperature. Combined NMR and MD simulation studies have confirmed that molecules could adopt conformations within confined spaces different from that in solution, opening opportunities to modulate chemical behavior of guest molecules.

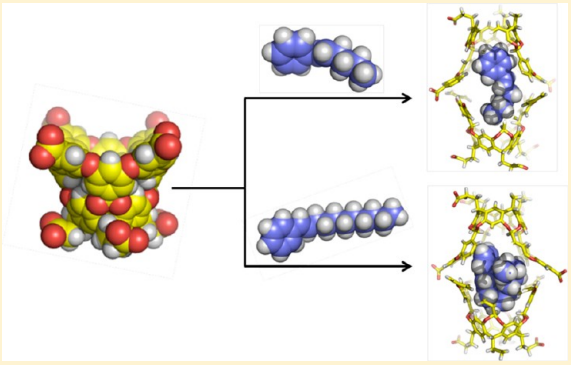

INTRODUCTION

In this study we are concerned with conformations of hydrocarbons of varied lengths and unsaturation within a deep cavity cavitand known by the trivial name "octa acid" (OA; Figure 1).[1] Depending on the size, shape, and polarity of guest molecules, OA is known to form host−guest complexes of compositions 1:1, 2:1, and 2:2 in water.[2] Compared to cavitands such as cyclodextrins, cucurbiturils, and calixarenes, OA capsular assemblies (2:1 and 2:2; host:guest) provide better confinement to the encapsulated guest molecules.[3−9] For the past eight years we have been utilizing the OA capsular assemblies for manipulating the excited state properties of organic guest molecules. In these studies we have observed that the outcome of the reactions depends on the orientation and/or conformation of guest molecules within the capsule.[6,9,10] For example, when OA encapsulated α-alkyl dibenzyl ketone was irradiated, depending on the alkyl chain length different products were obtained.[6] On the basis of the existing knowledge, we could not have predicted such an outcome beforehand. As illustrated in Figure 2a, ^{1}H NMR spectral analyses suggested that the molecule depending on the alkyl chain length adopted different conformations within the OA. A similar observation was made in the case of *p*-alkyl dibenzyl ketone.[9,10] Once again ^{1}H NMR spectral analyses revealed that the molecules adopt different conformations within the OA capsule (Figure 2b). In the case of α-alkyl cyclohexyl phenyl ketone products different from that in solution were observed within OA. While ^{1}H NMR spectral analyses suggested that the molecule adopts the same conformation both in solution and within OA, only molecular modeling studies revealed that the rotational mobility of the key C−C bond was restricted within OA. Interestingly, chiral induction during photocylization of pyridones and tropolones occurred within the OA capsule but not in solution.[11,12] Once again the extent of chiral induction was dependent on the site to which the alkyl group was present. The reason for the dependence was elucidated from ^{1}H NMR studies. Clearly, the orientation of guests controlled by the alkyl group made a significant difference on the extent of chiral induction (21−92%).[11,12] Even more importantly, observation relates to our ability to trap a high energy conformer of alkoxy-substituted piperidines within the OA capsule.[13] In this example, the conformer that is preferred within the OA capsule was dependent on the alkyl chain length (Figure 2c). While we have been successful in achieving unique chemistry within the confined spaces of the OA capsule, most of these discoveries were serendipitous in nature. Each example became a "show and tell" as one could not have predicted how a molecule would be accommodated within the OA capsule.

The above deficiency of unpredictability prompted us to undertake a detailed systematic investigation on how a

Received: September 12, 2012
Revised: November 20, 2012
Published: December 6, 2012

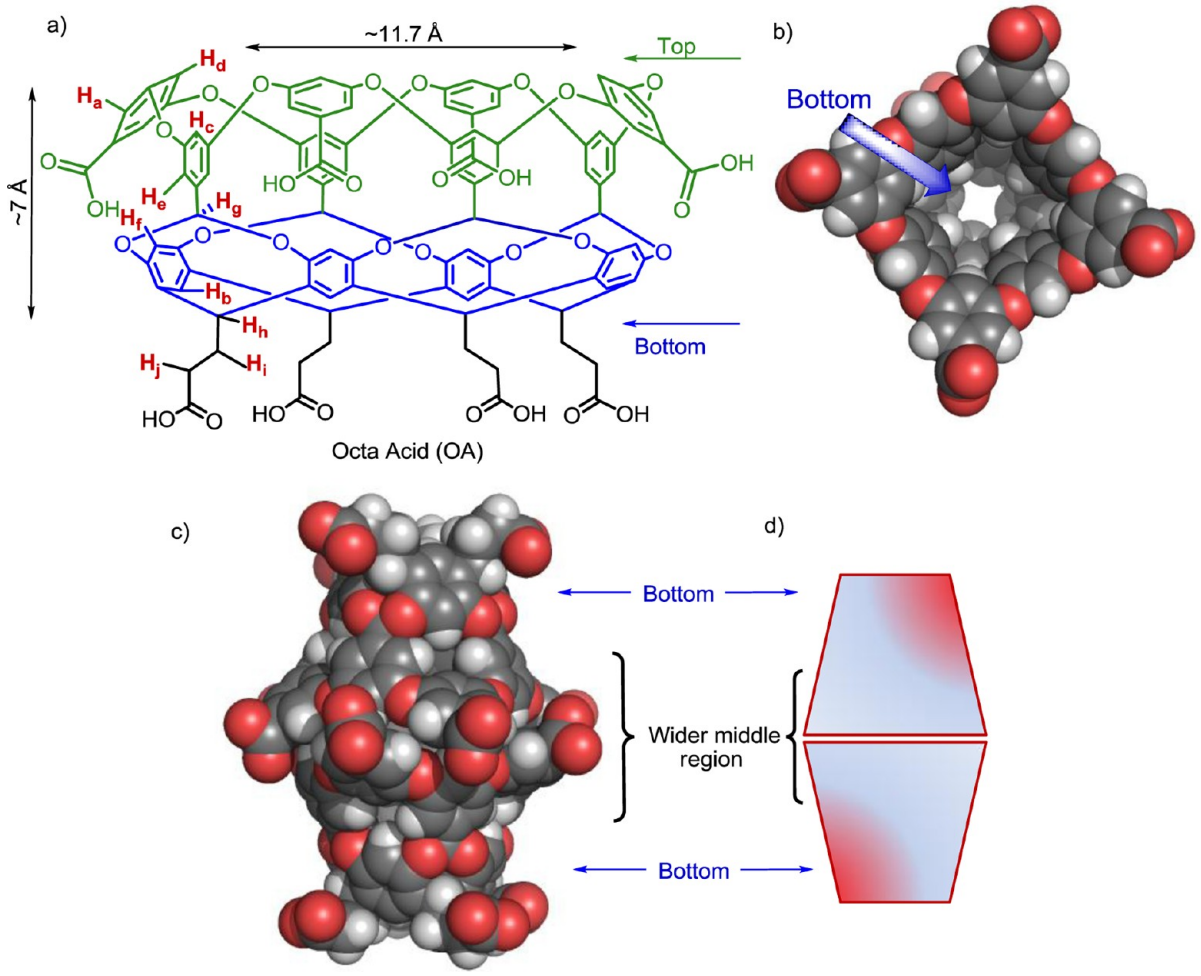

Figure 1. Chemical structure of (a) OA with dimensions, (b) a CPK model of the OA cavitand, (c) a CPK model of the OA capsule in the presence of a guest, and (d) a cartoon representation showing different parts of the OA capsule. The diameter and length of OA were calculated from the equilibrated structure of OA after 40 ns of MD simulation utilizing the OPLS-AA force field.

molecule with a long alkyl chain would adopt itself within the OA capsule. Our goal is to develop a simple model by which one can predict the photochemical outcome within a confined space rather than offer an ad hoc explanation after each interesting observation. In this study we have attempted to probe the conformational preference of model hydrocarbons of different chain lengths within the OA capsules through ^{1}H NMR experimental investigations and molecular dynamics (MD) simulations. As model systems we have chosen alkenes (**1a**−**1f**), alkynes (**2a**−**2d**), and alkanes (**3a**−**3f**) within the OA capsule (Scheme 1). There has been considerable interest in probing the conformations of molecules with alkyl chains within the confined spaces of cucurbiturils, Fujita's Pd host, and Rebek's hydrogen bonded assemblies.[14−22] Most of these studies involve ^{1}H NMR spectral analyses. We have undertaken combined ^{1}H NMR experimental and MD simulations with the belief that the complementary nature of these two approaches would provide a comprehensive understanding of the conformational preference within the confined space of a OA capsule. While ^{1}H NMR spectral analyses provide information concerning the location and geometry of guests within the host OA at equilibrium, visualization of real time MD simulation frames provides an understanding of how the guest molecule attains this equilibrium structure. Thus ^{1}H NMR spectral and MD simulation studies are complementary in nature and help us gain an in-depth knowledge of the host−guest complexation process in water. Although the molecules we have chosen for the current study are not photoactive, we believe that the information they provide will help us predict the photochemical outcome of similar molecules with photoactive groups.

In general, the most predominant conformation of an alkane in solution is the one with a fully extended carbon chain. Each kink in the carbon chain generally introduces steric interactions and increases the energy by ∼0.55 kcal/mol.[23] For example, ethane, the simplest alkane, has several conformations differing by small changes in torsion angles (the angle between the planes H−C−C and C−C−H).[23] The most stable conformation has a torsion angle of 180°. The difference in potential energy between staggered and eclipsed conformers (torsion angle 0°) of ethane is 2.9 kcal/mol, with the staggered being more stable. However, a highly energetically unfavorable conformer in solution could become stable when confined within small spaces provided by natural receptors and synthetic hosts.[14,16,17,19,20,24−29] In these media the unfavorable steric problems are overcome by maximization of contact with the walls of the hosts through weak interactions such as van der Waals, hydrogen bonding, $\pi-\pi$ interactions, etc. In this study we have probed the conformational preference of alkenes (**1a**−**1f**), alkynes (**2a**−**2d**), and alkanes (**3a**−**3f**) within the OA capsule by combining ^{1}H NMR experiments with classical MD

dx.doi.org/10.1021/jp3090815 | J. Phys. Chem. B 2013, 117, 398−407

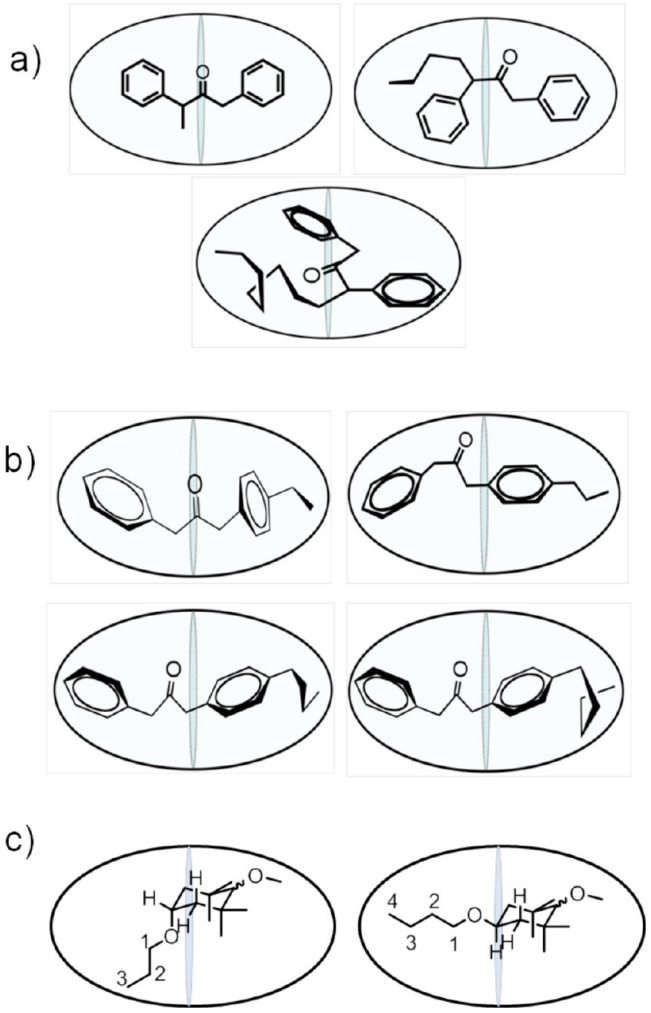

Figure 2. Schematic representations of encapsulated guest molecules within OA capsule. (a) α-Alkyl dibenzyl ketones within OA capsule, (b) *p*-alkyl dibenzyl ketones within OA capsule, and (c) alkoxy-substituted piperidines within OA capsule. Note the propoxy group is in axial position while butoxy is in equatorial position. In solution both are in equatorial position.

simulations. The NMR technique can provide useful information regarding the location, orientation, and kinetics of binding of a guest molecule with OA. MD simulations link both structure and dynamics by enabling the exploration of the conformational energy landscape accessible to molecules. In this study, the main emphasis of all MD simulations was to investigate dynamic transformations of the host–guest complexes and the correlation between the computed dynamics and the information obtained from the NMR experiments. Combined ^{1}H NMR and MD simulation studies we have undertaken have demonstrated that the conformational preference of a hydrocarbon within the OA capsule depends on the alkyl chain length as well as the group (H_2C-CH_2, HC=CH, and C≡C) that is adjacent to the phenyl group in 1-phenyl hydrocarbons. Results of these studies are discussed below.

RESULTS AND DISCUSSION

Guests examined in this study were synthesized by known procedures as detailed in the Supporting Information. Characterization of host–guest complexes was performed by one- and two-dimensional (1D and 2D) ^{1}H NMR spectroscopy (correlation spectroscopy (COSY), nuclear Overhauser effect spectroscopy (NOESY), rotating-frame Overhauser effect spectroscopy (ROESY), and the pulsed-field-gradient spin echo (PGSE) technique.[30] Under our experimental conditions ^{1}H NMR spectra did not contain signals for free OA and uncomplexed guest molecules, suggesting that in the ^{1}H NMR time scale there were no free guest and host molecules in solution.

MD simulations were performed using the following multistep strategy. In the first step, a three-dimensional structure of OA was constructed and optimized using the Merck molecular force field[31] included in the SPARTAN 04 program. This structure was further equilibrated through 40 ns all-atom MD simulations in an explicit aqueous solution utilizing the OPLS-AA force field[32,33] and GROMACS program.[34,35] The structures of the guest molecules were constructed and optimized using the Chembio3D program and MM2 force field.[36] In the next step, all guest molecules were docked inside the most representative structure provided by the previous 40 ns MD simulation of the OA capsule utilizing the AutoDock Vina program.[37] The most stable conformations provided by the docking procedure were energy minimized using the OPLS-AA force field as implemented in the GROMACS program. The minimized conformations were further utilized as the starting structures for 40 ns all-atom MD simulations in an explicit aqueous solution. The structural characteristics of the equilibrated structures provided by these simulations were compared with the NMR data.

Guest Inclusion within Hosts. Upon inclusion of guest molecules within OA, the ^{1}H NMR signals of all guest molecules were upfield shifted due to magnetic shielding resulting from benzene rings that form the framework of OA (Figures 3, 4, and 5). In this context, a careful look at the upfield region (0 to −4 ppm) of the NMR spectra is in order. The methyl signals of **1a**–**1d**, **2a**, **2b**, and **3a**–**3f** were upfield shifted to below δ = −2.5 ppm ($\Delta\delta$ = ∼ −4.0; $\Delta\delta$ is $\delta_{CDCl_3} - \delta_{OA\ complex}$) (Figures 3–5). On the other hand, in the cases of **1e**, **1f**, **2c**, and **2d**, the $\Delta\delta$ values were slightly less (∼ −3.0). The observed upfield shift of ^{1}H NMR signals is a clear indication that these guest molecules were included within OA.

Determination of Host–Guest Stoichiometry. By ^{1}H NMR titration experiments the host–guest ratios for alkenes (**1a**–**1f**), alkynes (**2a**–**2d**), and alkanes (**3a**–**3f**) within the OA capsule were determined to be 2:1 (Figures S1–S16 in the Supporting Information). During titration experiments, addition of up to 0.5 equivalent of guest to the host solution showed no signals due to unbound guest molecules in the ^{1}H NMR spectrum. Further addition of the guest resulted in turbid solution and unbound guest signals, suggesting that the host–guest ratio for a stable complex was 2:1. As expected, the measured diffusion coefficients of the complexes by diffusion ordered spectroscopy (DOSY) experiments were lower (1.08×10^{-10}–1.25×10^{-10} m^2/s) than that of free OA (1.73×10^{-10} m^2/s) (Table S1 in the Supporting Information).[38] Moreover, the diffusion constants were comparable to the 2:1 host–guest complexes formed between OA and other guests previously reported from our group.[2,6] In DOSY spectra, both host and guest signals exhibited similar diffusion coefficients, confirming that the supramolecular complexes formed in water were stable in the NMR time scale.

dx.doi.org/10.1021/jp3090815 | J. Phys. Chem. B 2013, 117, 398–407

Scheme 1. Structures of the Guests 1a−3f Used in This Study[a]

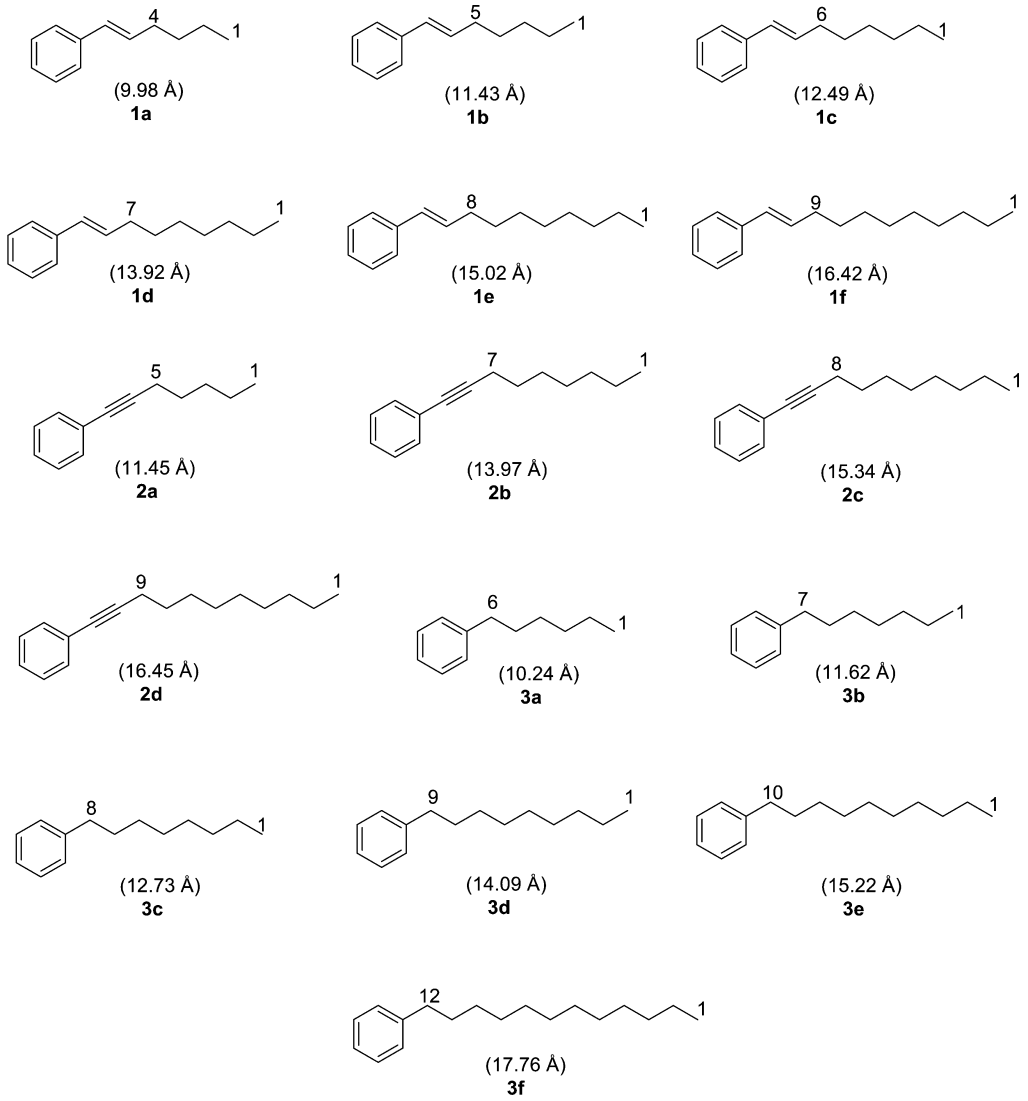

[a]The lengths of the molecules in their extended form are provided in parentheses (dimension of each structure refers to atom-to-atom distance and does not include van der Waals radii). Lengths of the molecules were calculated by performing an energy optimization using the ChemBio3D program and MM2 force field.

Location of Guests within the OA Capsule. Analysis of the chemical shift of the CH_3 and adjacent two CH_2 groups (CH_3−CH_2−CH_2−) of the alkane chain for various guest molecules (Figure 6) provided an insight regarding their location within OA. The plot of chemical shift vs molecular length of OA complexes of **1a**−**1d**, **2a**, and **2b** indicated that the CH_3− group and two adjacent CH_2− groups were located at the narrower end of the capsule. As the length of the chain became longer, as in **1e**, **1f**, **2c**, and **2d**, these groups (CH_3 and the next two −CH_2 groups) occupied the wider middle region of the capsule. We believe that, in the former case, the molecules with dimensions less than the OA capsule (~14 Å, Figure 1 and Scheme 1) would remain in an extended form, whereas in the latter cases the molecules with chain lengths longer than the length of the OA capsule would not be able to fit in an extended form and therefore would be forced to kink (fold). This would place the CH_3 group and the two adjacent CH_2 groups above the narrower bottom of the capsule.

Mobility of Guest Molecules within the OA Capsule. OA has 10 different sets of protons that are designated with letters "a"−"j" in Figure 1. Assessment of the intermolecular ^1H−^1H NOE interactions of a guest molecule with seven protons (designated as H_a, H_b, H_c, H_d, H_e, H_f, and H_g) of OA help us gain an insight into the location and coiling of guest molecules inside the OA capsule. OA molecule has a fourfold symmetry. Depending on the nature and dynamics of the included guest molecule, the OA capsule as a whole could be symmetrical or unsymmetrical. The two halves of the capsule are equivalent when a symmetrical guest is encapsulated, but placement of an unsymmetrical guest would make the two halves of the capsule magnetically nonequivalent, generating two sets of ^1H NMR signals for chemically equivalent hydrogens on the top and bottom halves of the OA capsule. However, an unsymmetrical guest that is able to freely tumble inside the capsule in the NMR time scale would make the two halves of the capsule symmetrical.[39] The important point to note is that, in the complexes of **1a**−**1d**, most of the host signals are split into two (Figure 7). A similar splitting pattern was observed for encapsulated **2a** and **2b** (Figure 4), suggesting

dx.doi.org/10.1021/jp3090815 | J. Phys. Chem. B 2013, 117, 398−407

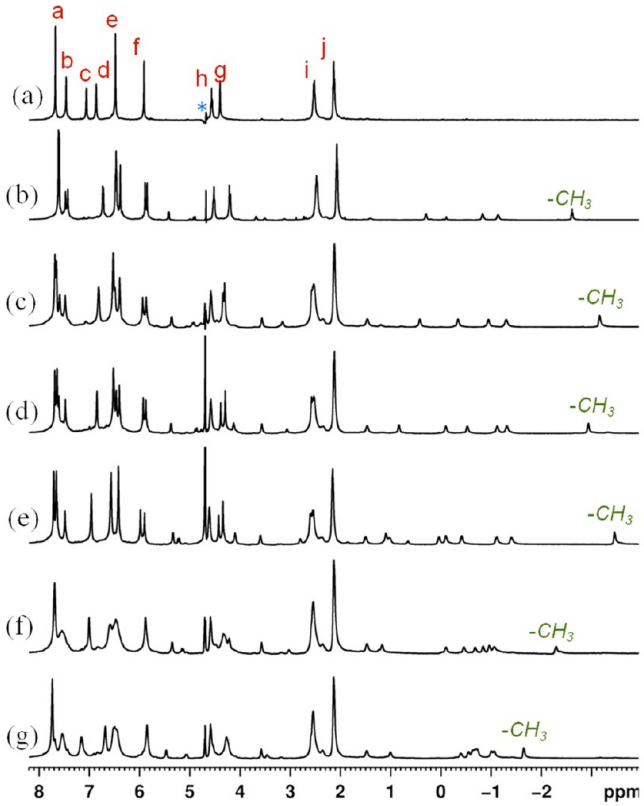

Figure 3. ^{1}H spectra (500 MHz, in sodium tetraborate buffer in D_2O) of (a) OA, (b) **1a**@OA_2, (c) **1b**@OA_2, (d) **1c**@OA_2, (e)**1d**@OA_2, (f) **1e**@OA_2, and (g) **1f**@OA_2. [OA] = 1 mM and [guest] = 0.5 mM. The asterisk (∗) indicates the signal due to residual water. $-CH_3$ indicates the signal of the methyl groups of **1a**−**1f** inside the OA capsule.

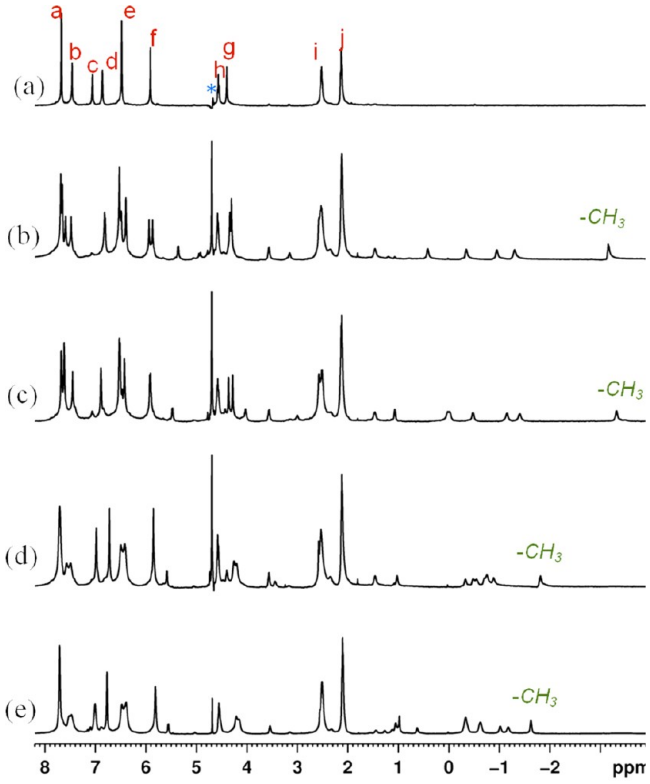

Figure 4. ^{1}H spectra (500 MHz, in sodium tetraborate buffer in D_2O) of (a) OA, (b) **2a**@OA_2, (c) **2b**@OA_2, (d) **2c**@OA_2, and (e) **2d**@OA_2. [OA] = 1 mM and [guest] = 0.5 mM. The asterisk (∗) indicates the signal due to residual water. $-CH_3$ indicates the signal of the methyl groups of **2a**−**2d** inside the OA capsule.

that in the presence of the above guest molecules two halves of the OA capsule are not identical in the NMR time scale. In these cases in the NOE spectra the aromatic hydrogens of the guest molecules interact with one set of "g" hydrogens whereas the aliphatic hydrogens of the guest molecules interact with another set of "g" hydrogens. This suggests that these molecules are encapsulated in such a manner that the methyl and phenyl groups are positioned within two different OA cavitands that form the capsule. Clearly in the NMR time scale these molecules do not freely tumble within the OA capsule.

In **1e**, **1f**, **2c**, and **2d** the host signals were broad at room temperature, suggesting that the guest molecules tumbled slowly in the NMR time scale within the capsule (Figure S17, Supporting Information). To examine the temperature dependence of guest tumbling within the capsule, ^{1}H NMR spectra were recorded at different temperatures. Figure 8 presents NMR spectra for **1f**@OA_2 complex between 278 and 308 K. Interestingly, signals for protons b, c, e, and g of OA split into two at 278 K. The broad host signals of **1f**@OA_2 at room temperature became sharper at higher temperatures. Analysis of NMR signals of guests with the saturated alkyl chain (**3a**−**3f**) showed a different behavior. Only one set of sharp signals for various protons of OA were recorded even after encapsulation of **3a**−**3f** within OA, suggesting that these guest molecules bearing flexible alkyl chains were able to rotate freely inside the OA capsule leading to symmetrization of the host signals into one.

Conformation of Guest Molecules within the OA Capsule. For all OA complexes of alkenes (**1a**−**1f**), alkynes (**2a**−**2d**), and alkanes (**3a**−**3f**), the extent of ^{1}H−^{1}H interaction of the methyl group with H_g's (located at the narrower end of the cavity) of the host provides information about the folding of the chain within the OA cavity. To begin with, the ^{1}H NMR signal due to the methyl group for all guest molecules was assigned based on integration of the signals due to host and guest molecules and COSY experiments. The smallest member of this series was *trans-β*-butylstyrene (**1a**, 9.98 Å). Based on the length of the molecule in comparison with the dimension of OA (length of the capsule is ∼14 Å), we expected **1a** to remain in an extended conformation within the OA capsule. The NOE interactions of the methyl group of **1a** with H_b and H_f of OA demonstrated that the group was positioned in the tapered bottom part of OA (Figure 9). Moreover, the intensity of NOE interactions of H_g and H_f with methylene hydrogens of **1a** gradually decreased from C_i to C_{i+2} (C_i denotes the methyl group). A similar type of NOE correlation was observed for **1b**, **1c**, and **1d** (Figures S18, S19, and S20 in the Supporting Information). These observations suggested that the hydrocarbon chains of the above included guest molecules were likely to be accommodated in an elongated conformation within the cavity, with methyl groups positioned closer to the tapered lower part of OA. The most representative structures derived from MD simulations also supported this conclusion (**1a**@OA_2 and **1d**@OA_2 in Figure 10). A closer look at the 1D ^{1}H NMR spectra and 2D COSY spectra of **1a**−**1d**@OA_2 revealed that the hydrogens on phenyl groups of the encapsulated guests were highly upfield shifted (Figures S21−S24 in the Supporting Information). A similar trend was observed for **2b**. The cross peaks between methyl

dx.doi.org/10.1021/jp3090815 | J. Phys. Chem. B 2013, 117, 398−407

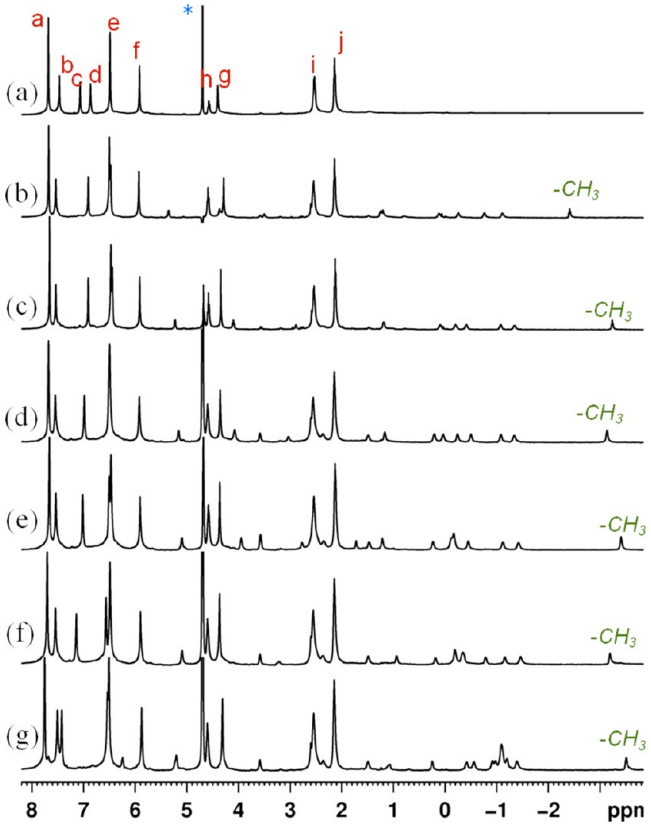

Figure 5. ^{1}H spectra (500 MHz, in sodium tetraborate buffer in D_2O) of (a) OA, (b) **3a**@OA_2, (c) **3b**@OA_2, (d) **3c**@OA_2, (e) **3d**@OA_2, (f) **3e**@OA_2, and (g) **3f**@OA_2. [OA] = 1 mM and [guest] = 0.5 mM. The asterisk (∗) indicates the signal due to residual water. $-CH_3$ indicates the signal of the methyl groups of **3a**−**3f** inside the OA capsule.

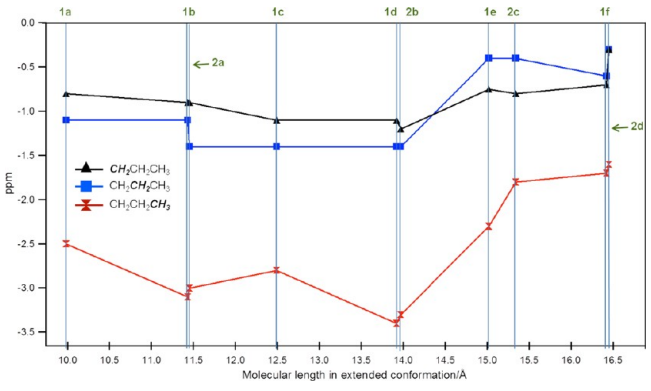

Figure 6. Plot of chemical shifts (ppm) of methyl and methylene groups for **1a**−**1f**@OA_2 and **2a**−**2d**@OA_2 versus the molecular length of the guests in their extended conformation.

group and H_b, H_f, and H_g of **2b**@OA_2 are shown in Figure S25 in the Supporting Information. The important point to note is that the hydrogens at C_1 and C_2 showed strong NOE correlation with H_e of OA, whereas hydrogens attached to carbons C_3, C_4, C_5, and C_6 exhibited correlations with H_d of OA. Moreover, the intensity of NOE interactions between methylene hydrogens with H_g gradually decreased from C_2 to C_5, indicating that the C_5 group was farther from H_g. Among the three different hydrogens of the phenyl group, the para hydrogen was the most upfield shifted ($\delta \sim 2.6$ ppm). This observation suggested that this hydrogen was positioned at the

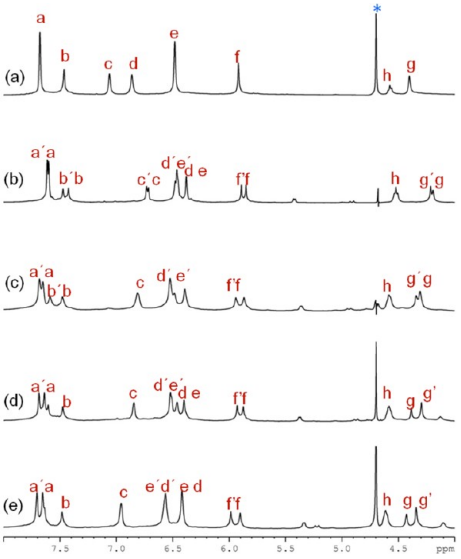

Figure 7. Partial ^{1}H spectra (500 MHz, in sodium tetraborate buffer in D_2O) of (a) OA, (b) **1a**@OA_2, (c) **1b**@OA_2, (d) **1c**@OA_2, and (e) **1d**@OA_2. [OA] = 1 mM in 10 mM sodium tetraborate buffer and [guest] = 0.5 mM. The asterisk (∗) indicates the signal due to residual water. Selected resonances of OA are labeled from "a" to "h".

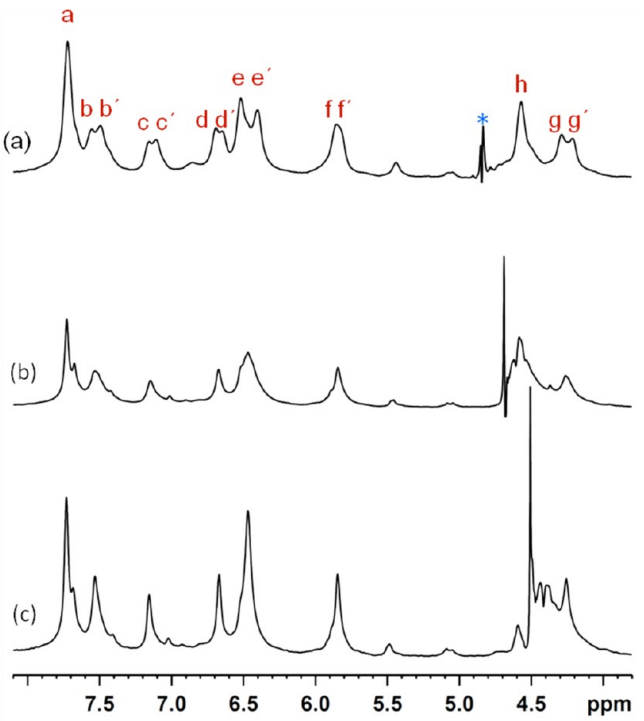

Figure 8. Partial ^{1}H spectra of **1f**@OA_2 (400 MHz, [OA] = 1 mM in 10 mM sodium tetraborate buffer, [OA]:[**1f**] = 1:0.5) of at (a) 278, (b) 298, and (c) 308 K. The asterisk (∗) indicates the signal due to residual water. Selected resonances of OA are labeled from "a" to "h".

tapered bottom part of the OA cavitand (Figure S26 in the Supporting Information). In addition to that, signals due to alkene hydrogens were observed in the region of δ = 4.2−4.5 ppm. A significantly less upfield shift of alkene hydrogens (δ = 4.2−4.5 ppm) indicated that they were located in the wider middle region of the OA capsule. The structures provided by MD simulations suggested that molecules with length > 15 Å may be too long to be encapsulated in the cavity in extended

dx.doi.org/10.1021/jp3090815 | J. Phys. Chem. B 2013, 117, 398−407

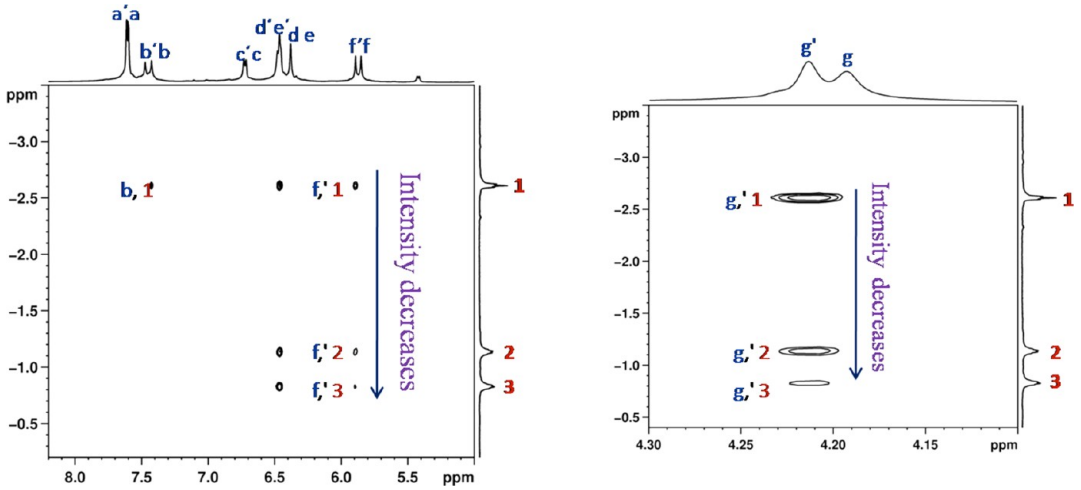

Figure 9. 2D NOESY (500 MHz, in sodium tetraborate buffer in D_2O) partial spectrum of **1a**@OA_2. [OA] = 5 mM in 50 mM sodium tetraborate buffer and [guest] = 2.5 mM. Aromatic resonances of the host are labeled from "a" to "g" (left). The intensity of NOE interaction between aliphatic hydrogens of **1a** with $H_{f'}$ and $H_{g'}$ of OA decreases with distance (right).

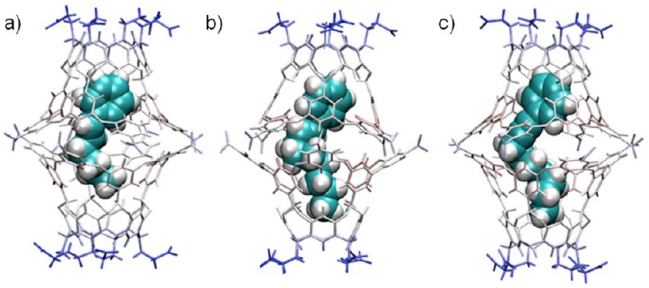

Figure 10. The most representative structures obtained from MD simulation (GROMACS, OPLS-AA force field) showing the orientation of different guest molecules inside the OA capsule. (a) **1a**@OA_2, (b) **1d**@OA_2, and (c) **2b**@OA_2.

conformations. Therefore, guest molecules such as **1e** (15.02 Å), **1f** (16.42 Å), **2c** (15.34 Å), and **2d** (15.34 Å) adopted a folded conformation in order to fit inside the OA capsule.

According to ^{1}H NMR spectra, the complexation induced chemical shifts for the methyl groups of **1e** and **1f** were $\Delta\delta$ = −3.4 and −2.48, respectively. However, the position of the C═C bond was in the wider middle region of the OA capsule, similar to the small guest molecules in this series. An inspection of NMR spectra of **1e**@OA_2 and **1f**@OA_2 revealed that the para hydrogen of the phenyl group in **1f** is less upfield shifted than that in **1e** (Figures S27 and S28 in the Supporting Information). Examination of complexes of **1e** and **1f** by 2D NOESY showed strong NOE cross peaks between the methyl groups with H_c and H_d of OA, which are present at the wider middle region of the OA capsule (Figure S29 in the Supporting Information). On the other hand, for **1f**@OA_2 complex the weak NOE cross peaks between the hydrogens attached to carbons C_5, C_6, and C_7 and H_g of OA demonstrate that this portion of the alkyl chain is located close to the tapered bottom part of the OA cavitand. Also, the NOE correlations between H_d of OA and most of the aliphatic hydrogens of **1e** and **1f** suggest that the aliphatic chains are folded in the wider middle region of the capsule. Similar results were obtained for **2c** (15.34 Å) and **2d** (16.45 Å). In the case of **2c**@OA_2, correlation between H_d and H_c of OA and aliphatic hydrogens of the chain was observed. No correlations between H_f and H_b and the hydrogens of the aliphatic chain of **2c** were noticed by NOESY. However, a very weak correlation between the methyl group and H_g was observed. All these observations suggested that the aliphatic chain of **2c** is located in the wider middle region of the capsule. Strong NOE correlations between H_d and aliphatic hydrogens of OA support this model (Figure S30 in the Supporting Information). A slightly longer alkyl chain of **2d** also folds upon encapsulation. Figure S31 in the Supporting Information shows a partial ROESY spectrum of the **2d**@OA_2 complex. There are strong intermolecular NOE cross peaks between hydrogens of the aliphatic chain and H_c and H_d of OA. In this context, the chemical shifts of hydrogens at the 5 and 6 positions of the aliphatic chain were noticeable (for COSY spectra see Figures S32 and S33 in the Supporting Information). As the aliphatic chain has taken the form of a loop, the middle region of it remains buried in the deep cavity of OA, showing NOE correlations between H_g and hydrogens on C_5, C_7, and C_4 of the chain. These results in conjunction with structures provided by MD simulations suggested that the alkyl chains of these four guest molecules remained folded within the OA capsule (Figure 11).

A different scenario emerged for the OA encapsulated saturated alkyl chains with a phenyl head group. In the case of **3a** (the shortest member in this series, length 10.24 Å), the ^{1}H NMR signal due to the methyl group appeared at δ = −2.4 ppm. The analysis of the complexation induced chemical shift ($\Delta\delta$) for the rest of the guests revealed that the methyl groups were most highly upfield shifted (−2.3 to −3.5 ppm). This observation indicated that the methyl groups were deeply buried inside the OA capsule. The signals due to methylene hydrogens on the aliphatic chain were distinctly separate for **3a**−**3e**, but it was not so for **3f** (Figures S34 and S35 in the Supporting Information). With the help of molecular dynamics simulation, we examined the conformational preferences of **3d** and **3f** within OA: **3d** has an intermediate and **3f** has the longest alkyl chain substituent among **3a**−**3f**. Two-dimensional NOESY NMR experiments and molecular modeling showed that **3d** is encapsulated, positioning the long alkyl tail in the tapering end of the OA cavitand (Figure 12). This phenomenon was common for the guest molecules with unsaturated alkyl chains of lengths less than 15 Å. The chemical shift of the aromatic head group of the guest indicates that it is

dx.doi.org/10.1021/jp3090815 | J. Phys. Chem. B 2013, 117, 398−407

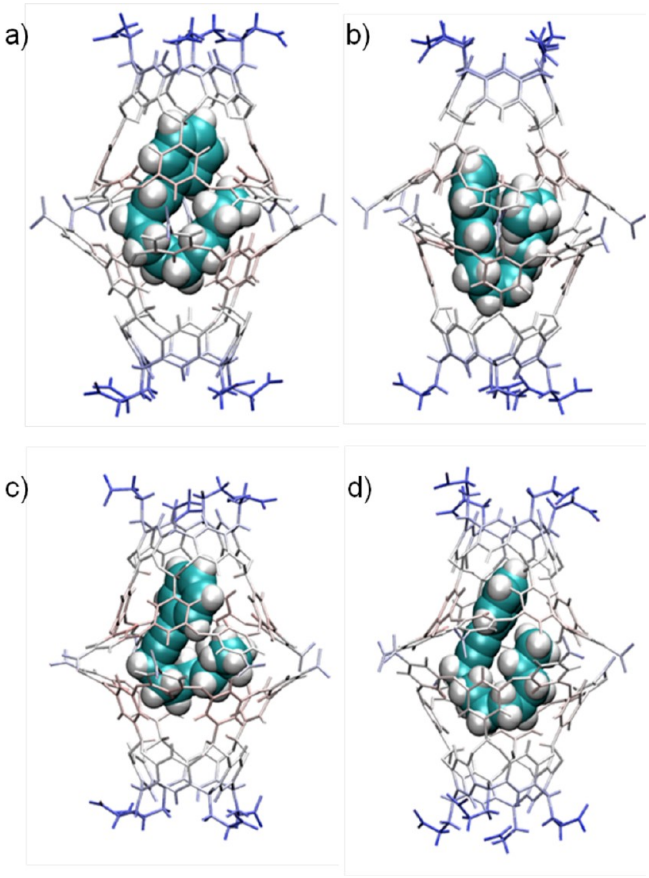

Figure 11. The most representative structures obtained from MD simulation (GROMACS, OPLS-AA force field) showing the orientation of different guest molecules inside the OA capsule. (a) **1e**@OA_2, (b) **1f**@OA_2, (c) **2c**@OA_2, and **2d**@OA_2.

deeply buried inside the OA cavity. This result was similar to those for **1a**−**1d** and **2b**−**2d**.

An interesting result was observed in the case of **3f**. The equilibrated structure provided by MD simulations showed that the bulky benzene rings were located in the wider middle region of the OA capsule, leading possibly to a $\pi-\pi$ type interaction with the benzene rings of the host. Plasticity of the alkyl chain enables the molecules to bend in a favorable conformation inside the OA capsule. A very clear scenario was obtained after examining the 2D NOESY data of **3f**@OA_2 complex (Figure 13).

The methyl group of **3f** showed NOE correlations with H_g, H_b, H_f, and H_e of OA. Among these interactions the one with H_g was highly intense, which indicated the proximity of the methyl group to H_g of OA. Also, hydrogens at C_2, C_3, and C_4 correlate with H_e but hydrogens at C_7, C_8, and C_{11} of the chain correlate with H_d of OA. No correlation between the methyl group and H_c/H_d of the host was observed. The NOE interaction between H_d of OA and aromatic hydrogens of the guest indicates that the aromatic head group was positioned in the wider middle region of the OA capsule. This observation suggested that the methyl end of the alkyl chain was held at the tapering end of the OA cavitand, whereas the upper head group was located at the wider middle region of the capsule. Most likely, the unanticipated bending was overcome by maximization of contacts with the walls of the cavitand. Because rigid, nonrotatable double and triple bonds hinder bending of the alkyl chain, this kind of folding was not observed with **1a**−**1f** and **2a**−**2d** as guests.

The trajectories derived from the MD simulations elucidated the mechanisms of host−guest complexation at the atomic level. In particular, they revealed both the dynamics and plasticities of the guest molecules as they tried to attain the thermodynamically most stable conformation inside the hydrophobic microenvironment of the host. The movies exhibiting these processes are provided in the Supporting Information, and the key observations from them are discussed below.

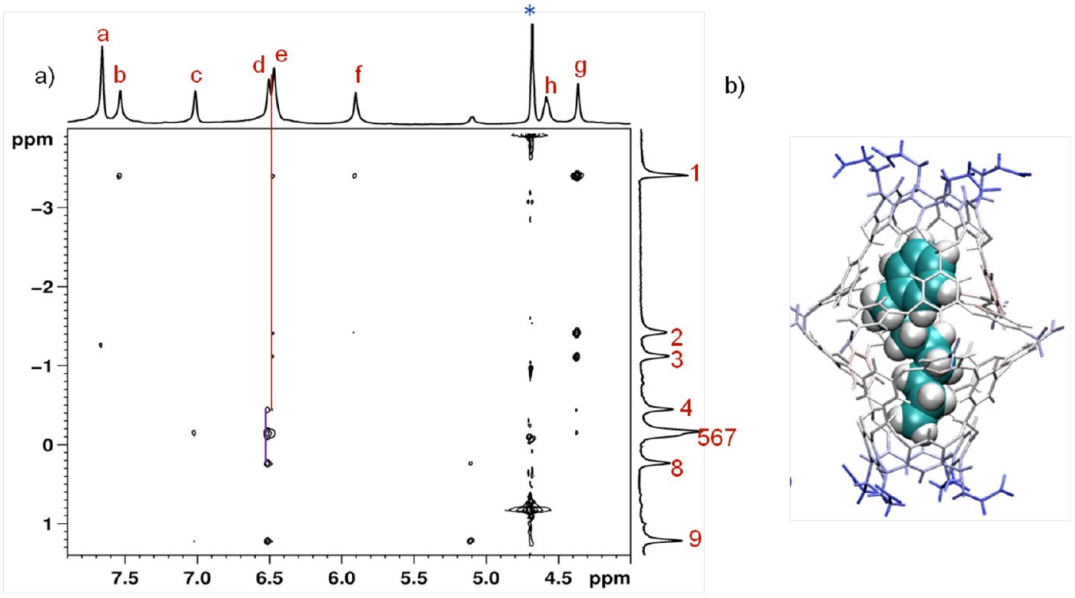

Figure 12. 2D NOESY (500 MHz) partial spectrum of (a) **3d**@OA_2. [OA] = 5 mM in 50 mM sodium tetraborate buffer and [guest] = 2.5 mM. Aromatic resonances of the host are labeled from "a" to "h" and aliphatic protons of the guest from "1" to "9". (b) The most representative structure obtained from MD simulation (GROMACS, OPLS-AA force field) shows the folding of **3d** inside the OA capsule.

dx.doi.org/10.1021/jp3090815 | J. Phys. Chem. B 2013, 117, 398−407

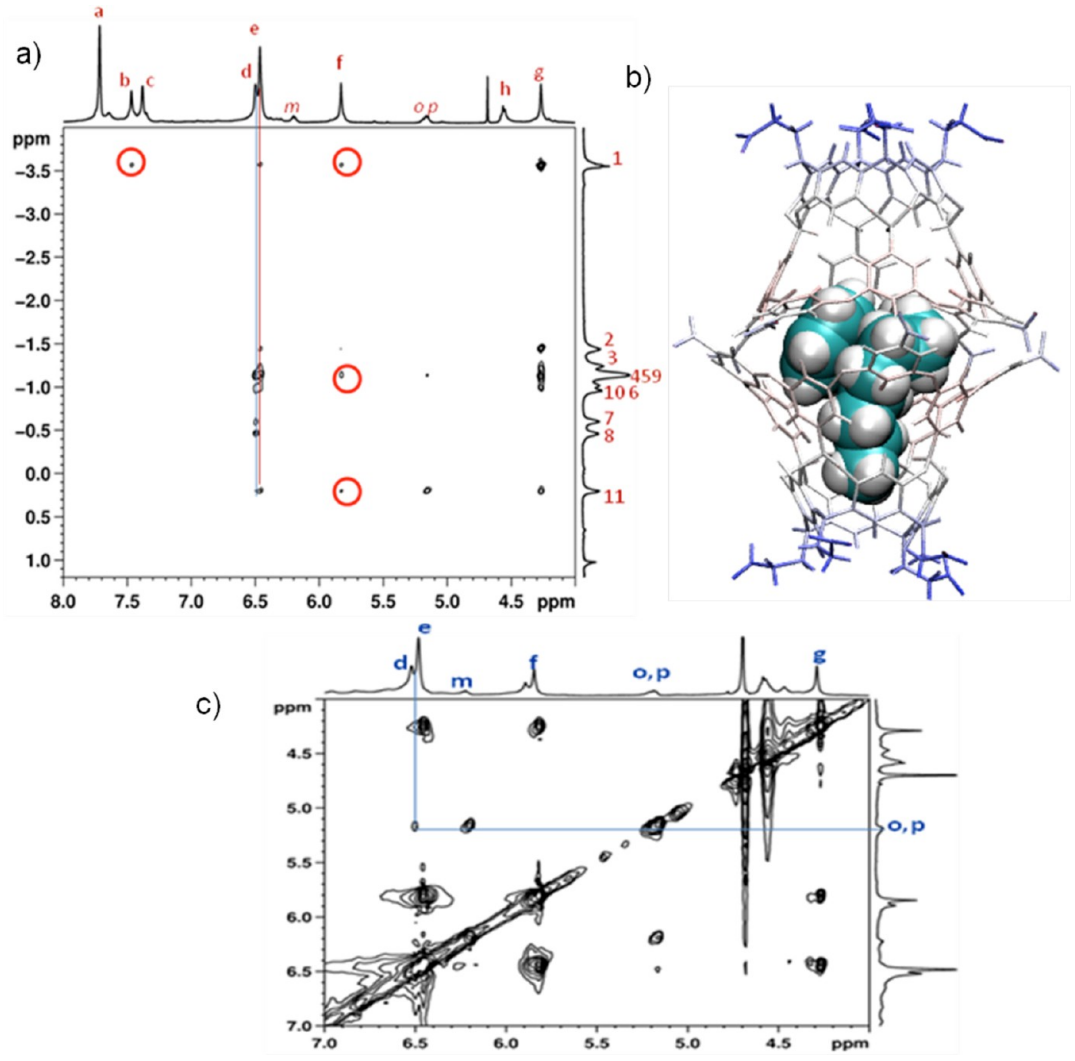

Figure 13. 2D NOESY (500 MHz) partial spectrum of (a) **3f**@OA_2. [OA] = 5 mM in 50 mM sodium tetraborate buffer and [guest] = 2.5 mM. Aromatic resonances of the host are labeled from "a" to "g", and aliphatic protons of the guest are labeled from "1" to "11". (b) The most representative structure obtained from MD simulation (GROMACS, OPLS-AA force field) shows the folding of **3d** inside the OA capsule. (c) NOE interaction between H_d of OA aromatic hydrogens of the guest.

For instance, both 1D and 2D NMR and MD simulations showed that *trans*-butylstyrene (**1a**) and *trans*-heptylstyrene (**1d**) with their short alkyl chains (9.98 and 13.92 Å, respectively) remained in the elongated forms within the OA capsule. An analysis of the corresponding trajectory (SI_movie1 and SI_movie2 in the Supporting Information) exhibited that these molecules maintained this stable conformation throughout the simulation. Rather interestingly, a slight elongation, by 1.10 Å, of the alkyl chain in *trans*-octylstyrene (**1e**) was found to force it into a folded structure inside the OA capsule. It is worth mentioning that in the starting structure of the simulation this molecule was in the extended form. In the first 10 ns of the simulation, it folded and twisted and placed the alkyl chain in the broader middle region of the capsule. After achieving this conformation, it remained in this form for the rest of the simulation (SI_movie3 in the Supporting Information). The *trans*-butylstyrene (**1a**) and heptylstyrene (**1d**) molecules showed similar dynamic fluctuations.

In the case of heptylphenylacetylene (**2b**), with the chain length of 13.97 Å, the initial docked structure was also in an extended form. However, within 0.1 ns of the simulation the alkyl chain started to fold. After numerous events of folding and unfolding in the first few nanoseconds, this chain finally settled into the tapered cavity of the OA and remained that way for the rest of the trajectory (SI_movie4 in the Supporting Information). In this conformation the molecule maximized interactions with the walls of the host. For **2c** (chain length 15.34 Å) and **2d** (chain length 16.45 Å) the longer lengths prevented the alkyl chains from staying in the extended forms and they remained in the folded states for the entire course of the simulation (SI_movie5 and SI_movie6 in the Supporting Information).

On the other hand, the alkyl chains of nonylbenzene (**3d**) and dodecylbenzene (**3f**) underwent a series of conformational changes (SI_movie7 and SI_movie8 in the Supporting Information). For **3d** the phenyl moiety momentarily occupied multiple locations inside the OA cavity, while for **3f** it was more rigid and always stayed in the broader middle region.

These movies explicitly exhibited the mechanisms followed by the guest molecules to overcome steric constraints and attain the most stable thermodynamic conformations inside the OA cavity.

dx.doi.org/10.1021/jp3090815 | *J. Phys. Chem. B* 2013, 117, 398−407

CONCLUSIONS

In this study, we have combined two complementary techniques, NMR spectroscopy and molecular dynamics simulations, to investigate the binding mechanisms of a series of hydrocarbons with varying lengths inside the OA capsule. Our results explicitly indicated that the folding of these hydrocarbons inside the OA cavity was determined both by the lengths of their alkyl chains and by their chemical characteristics (H_2C-CH_2, HC═CH, and C≡C). It was found that the flexible alkyl chains were capable of adopting some unusual conformations inside the hydrophobic microenvironment of the OA capsule that would be inaccessible to them in solution. These thermodynamically unstable states in solution are stabilized by specific interactions (C−H/π and $\pi-\pi$) between the guest and OA capsule. Due to their size the small molecules (<15 Å in length) can easily encapsulate in an extended form inside the capsule, but the ones with longer alkyl chains must fold in a specific manner to maximize their interactions with the host. It is noteworthy that their folding is also controlled by a double or triple bond containing a rigid functional group attached to them. Like a handle of a whip, this rigid group is observed to keep the phenyl head group in a fixed position in one of the OA cavitands and allows the aliphatic chain to fold and occupy the remaining cavity. In contrast, alkyl chains without such functional groups do not experience this restriction and fold only on the basis of size and shape complementarity and interactions with the host. The results reported in this study will enhance our understanding of the binding mechanisms and controlling factors of a wide range of chemically important hydrocarbons inside the hydrophobic environment of the OA capsule.

ASSOCIATED CONTENT

Supporting Information

Experimental details, synthesis procedures, details of molecular dynamics simulation, MPEG movies depicting 40 ns MD simulation trajectories, and additional 1D and 2D NMR spectra. This material is available free of charge via the Internet at http://pubs.acs.org.

AUTHOR INFORMATION

Corresponding Author

*E-mail: murthy1@miami.edu (V.R.); rpr@miami.edu (R.P.).

Notes

The authors declare no competing financial interest.

ACKNOWLEDGMENTS

V.R. is grateful to the National Science Foundation, USA, for generous financial support (CHE-0848017).

REFERENCES

(1) Gibb, C. L. D.; Gibb, B. C. *J. Am. Chem. Soc.* **2004**, *126*, 11408−11409.
(2) Jayaraj, N.; Zhao, Y.; Parthasarathy, A.; Porel, M.; Liu, R. S. H.; Ramamurthy, V. *Langmuir* **2009**, *25*, 10575−10586.
(3) *Molecular Encapsulation*; Brinker, U. H., Mieusset, J.-L., Eds.; John Wiley: Chichester, U.K., 2010.
(4) Masson, E.; Ling, X.; Joseph, R.; Mensah, L.-K.; Lu, X. *RSC Adv.* **2012**, *2*, 1213−1247.
(5) Lagona, J.; Mukhopadhyay, P.; Chakrabarti, S.; Isaacs, L. *Angew. Chem., Int. Ed.* **2005**, *44*, 4844−4780.
(6) Gibb, C. L. D.; Sundaresan, A. K.; Ramamurthy, V.; Gibb, B. C. *J. Am. Chem. Soc.* **2008**, *130*, 4069−4080.
(7) Gupta, S.; Choudhury, R.; Krois, D.; Wagner, G.; Brinker, U. H.; Ramamurthy, V. *Org. Lett.* **2011**, *13*, 6074−6077.
(8) Natarajan, A.; Kaanumalle, L. S.; Jockusch, S.; Gibb, C. L. D.; Gibb, B. C.; Turro, N. J.; Ramamurthy, V. *J. Am. Chem. Soc.* **2007**, *129*, 4132−4133.
(9) Sundaresan, A. K.; Ramamurthy, V. *Photochem. Photobiol. Sci.* **2008**, *7*, 1555−1564.
(10) Kulasekharan, R.; Choudhury, R.; Prabhakar, R.; Ramamurthy, V. *Chem. Commun.* **2011**, *47*, 2841−2843.
(11) Sundaresan, A. K.; Gibb, C. L. D.; Gibb, B. C.; Ramamurthy, V. *Tetrahedron* **2009**, *65*, 7277−7288.
(12) Sundaresan, A. K.; Kaanumalle, L. S.; Gibb, C. L. D.; Gibb, B. C.; Ramamurthy, V. *Dalton Trans.* **2009**, 4003−4011.
(13) Porel, M.; Jayaraj, N.; Raghothama, S.; Ramamurthy, V. *Org. Lett.* **2010**, *12*, 4544−4547.
(14) Tashiro, S.; Kobayashi, M.; Fujita, M. *J. Am. Chem. Soc.* **2006**, *128*, 9280−9281.
(15) Dolain, C.; Hatakeyama, Y.; Sawada, T.; Tashiro, S.; Fujita, M. *J. Am. Chem. Soc.* **2010**, *132*, 5564−5565.
(16) Ko, Y. H.; Kim, Y.; Kim, H.; Kim, K. *Chem. Asian J.* **2011**, *6*, 652−657.
(17) Ko, Y. H.; Kim, H.; Kim, Y.; Kim, K. *Angew. Chem., Int. Ed.* **2008**, *47*, 4106−4109.
(18) Purse, B. W.; Rebek, J. J. *Proc. Natl. Acad. Sci. U.S.A.* **2006**, *103*, 2530−2534.
(19) Trembleau, L.; Rebek, J. *Science* **2003**, *301*, 1219−1220.
(20) Scarso, A.; Trembleau, L.; Rebek, J. *J. Am. Chem. Soc.* **2004**, *126*, 13512−13518.
(21) Ajami, D.; Rebek, J. *J. Am. Chem. Soc.* **2006**, *128*, 15038−15039.
(22) Ajami, D.; Rebek, J. *Nat. Chem.* **2009**, *1*, 87−90.
(23) Eliel, E. L.; Wilen, S. H. *Stereochemistry of Organic Compounds*; Wiley: New York, 1994.
(24) Purse, B. W.; Rebek, J., Jr. *Proc. Natl. Acad. Sci. U.S.A.* **2006**, *103*, 2530−2534.
(25) Schramm, M. P.; Rebek, J. *Chem.—Eur. J.* **2006**, *12*, 5924−5933.
(26) Siering, C.; Torang, J.; Kruse, H.; Grimme, S.; Waldvogel, S. R. *Chem. Commun.* **2010**, *46*, 1625−1627.
(27) Udachin, K. A.; Enright, G. D.; Brouwer, E. B.; Ripmeester, J. A. *J. Supramol. Chem.* **2001**, *1*, 97−100.
(28) Wanjari, P. P.; Sangwai, A. V.; Ashbaugh, H. S. *Phys. Chem. Chem. Phys.* **2012**, *14*, 2702−2709.
(29) Zanotti, G.; Scapin, G.; Spadon, P.; Veerkamp, J. H.; Sacchettini, J. C. *J. Biol. Chem.* **1992**, *267*, 18541−18550.
(30) Gunther, H. *NMR Spectroscopy*; John Wiley: Chichester, U.K., 1992.
(31) Halgren, T. A. *J. Comput. Chem.* **1996**, *17*, 490−519.
(32) Jorgensen, L. W.; Tirado-Rives, J. *J. Am. Chem. Soc.* **1988**, *110*, 1658.
(33) Kaminski, A. G.; Friesner, A. R.; Tirado-Rives, J.; Jorgensen, L. W. *J. Phys.Chem. B* **2001**, *105*, 6474.
(34) Lindahl, E.; Hess, B.; Spoel, V. D. *J. Mol. Model.* **2001**, *7*, 306.
(35) Spoel, V. D.; Lindahl, E.; Hess, B.; Groenhof, G.; Mark, A. E.; Berendsen, J. C. H. *J. Comput. Chem.* **2005**, *26*, 1701−1718.
(36) Allinger, N. L. *J. Am. Chem. Soc.* **1977**, *99*, 8127−8134.
(37) Trott, O.; Olson, A. J. *J. Comput. Chem.* **2010**, *31*, 455−461.
(38) Cohen, Y.; Avram, L.; Frish, L. *Angew. Chem., Int. Ed.* **2005**, *44*, 520−554.
(39) Kulasekharan, R.; Jayaraj, N.; Porel, M.; Choudhury, R.; Sundaresan, A. K.; Parthasarathy, A.; Ottaviani, M. F.; Jockusch, S.; Turro, N. J.; Ramamurthy, V. *Langmuir* **2010**, *26*, 6943−6953.